Experiment 3

Scanning Fabry-Perot Interferometer

References

- *Optics* by E. Hecht; See Section 9.6 for the Fabry-Perot interferometer, and Section 14.2 for an overview of lasers.
- *An Introduction to Lasers and Masers* by A. Siegman; see Chapter 8 for an excellent discussion of optical resonators; see Sections 9.2 and 9.4 for treatments of Doppler broadening, laser oscillation frequencies, and the Lamb dip.
- *Optical Electronics* by A. Yariv; Chapters 4 through 7 are highly recommended; Chapter 4 discusses Fabry-Perot interferometers and optical resonators, Section 6.6 contains an insightful comparison between homogeneous and inhomogeneous line profiles and the effect on lasing, Section 6.8 explains the Lamb dip, and Section 7.5 describes the helium-neon laser and includes a neon atomic energy level diagram.
- "Scanning Spherical-Mirror Interferometers for the Analysis of Laser Mode Structure" by D. Sinclair (a scanned pdf copy is available on the course Sakai website); this technical bulletin is distributed by Spectra-Physics and provides a good introduction to most of the measurements performed in this experiment.
- *Quantum Physics of Atoms, Molecules, Solids, Nuclei, and Particles* by Eisberg and Resnick. Section 10-6 describes the Zeeman effect using Na as an example. While Ne is a neighbor of Na in the periodic table, the excited states of Ne are described by j-l coupling rather than LS coupling.

3.1 Introduction

In this experiment a Fabry-Perot interferometer with a resolving power of 10^7 will be used to examine the spectral profiles of two helium-neon lasers and to measure the Zeeman splitting of neon in one of these lasers. Our Fabry-Perot instrument has an optical cavity formed by two spherical mirrors arranged in the confocal configuration. The term "confocal" means that a point midway between the mirrors is the focal point of both mirrors. The Fabry-Perot interferometer transmits light whose wavelength is resonant with the cavity. To scan a spectrum, the distance between the mirrors is varied slightly by applying a ramp voltage to a piezoelectric crystal on which the mirrors are mounted. As the separation of the mirrors is varied, the wavelength of light transmitted by the interferometer varies, and the photodiode at the rear of the interferometer measures the transmitted intensity. Thus the output of the photodiode plotted versus the ramp voltage applied to the piezoelectric crystal yields the spectral profile of the incident laser beam.

Our Fabry-Perot instrument is called a "scanning confocal spherical mirror Fabry-Perot interferometer," or sometimes just an "optical spectrum analyzer." This class of instruments is routinely used to monitor the operating characteristics of lasers. In addition to providing an introduction to Fabry-Perot interferometers, this experiment involves a fair amount of laser physics including the principles of optical resonant cavities. The observation of the Zeeman splitting in neon also involves a good deal of atomic physics. Because much of the material in this experiment will be new to you, you will have to consult the references listed above in order to be productive in the laboratory.

3.2 Examining the Output Beam of the Uniphase Model 1125P HeNe Laser

Most of the first laboratory meeting will be spent learning to operate the Spectra-Physics Model 470 Scanning Fabry-Perot Interferometer (let's call it the "SF-P" for short). You will use the SF-P to examine the output of the Uniphase Model 1125P helium-neon laser. The Model 1125P has a plane-polarized, 5-mW output at 632.8 nm. The specifications say that more than 95% of its output power is in the TEM_{00} transverse (spatial) mode. The TEM_{00} mode possesses the familiar Gaussian distribution of intensity. (The intensity is proportional to $\exp\left(-2r^2/w^2\right)$ where r is the distance from the center of the beam spot and w is called the spot size (radius).)

A photo of the laser-interferometer setup appears in Fig. 3.1, and a sketch with electrical connections is included in Fig. 3.2. Power **On** the Hewlett-Packard Model 54603B digital oscilloscope and the Model 1125P laser. (The *unpolarized* Model 1125 should be housed inside the solenoid, and the *polarized* Model 1125P is probably sitting on the optical rail next to it.) Make sure the cable connections between the oscilloscope, the Spectra-Physics Model 476 Interferometer Driver (let's call it the Driver for short), and the SF-P agree with the connections sketched in Fig. 3.2. In order to familiarize yourself with the function of the Driver controls, perform the following

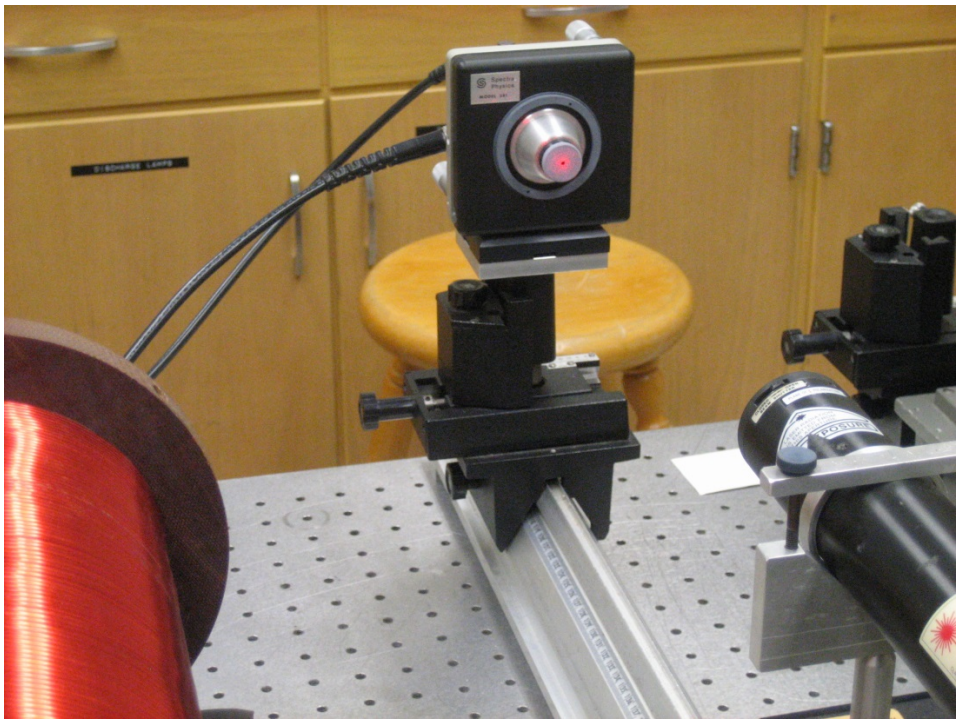

Figure 3.1: Photogaph of the Fabry-Perot (center-top) illuminated by the Uniphase 1125P (polarized) HeNe laser (bottom-right). The solenoid is visible at the lower left and houses the Uniphase 1125 HeNe laser.

exercises. (A copy of the Driver manual has been placed with the experimental equipment.)

1. Observe the high-voltage ramp applied by the Driver to the piezoelectric crystal; this ramp varies the spacing between the mirrors of the SF-P. To make this observation, disconnect the Driver high voltage output (200 to 300 volts) from the SF-P as sketched in Fig. 3.2, and connect it to the input of the 100× attenuator (the small box that is probably located on the oscilloscope cart). Connect the output of the attenuator to input 1 of the oscilloscope and change the horizontal display to "Main" instead of "XY" which is the setting used in Fig. 3.2. (Press "Main/Delayed" and select "Main" in the submenu appearing on the oscilloscope screen.) Now power **On** the Driver. Set the Driver SWEEP to FREE RUN and the SWEEP TIME to 0.01 sec (turn the TIME knob fully clockwise). Set the Driver DISPERSION to X2 with the VARIABLE knob set at midrange. Set the vertical gain of the scope to 1 V/div, and set the horizontal sweep to 5 ms/div. Observe the attenuated ramp on the oscilloscope screen. Play with the Driver CENTERING knob and notice that its effect is simply to increase or decrease the DC level of the high voltage ramp. Play with the Driver DISPERSION settings and notice that they control the amplitude of the ramp. When you think you understand the function of the DISPERSION and CENTERING controls on the Driver, power **Off** the Driver. Reconnect

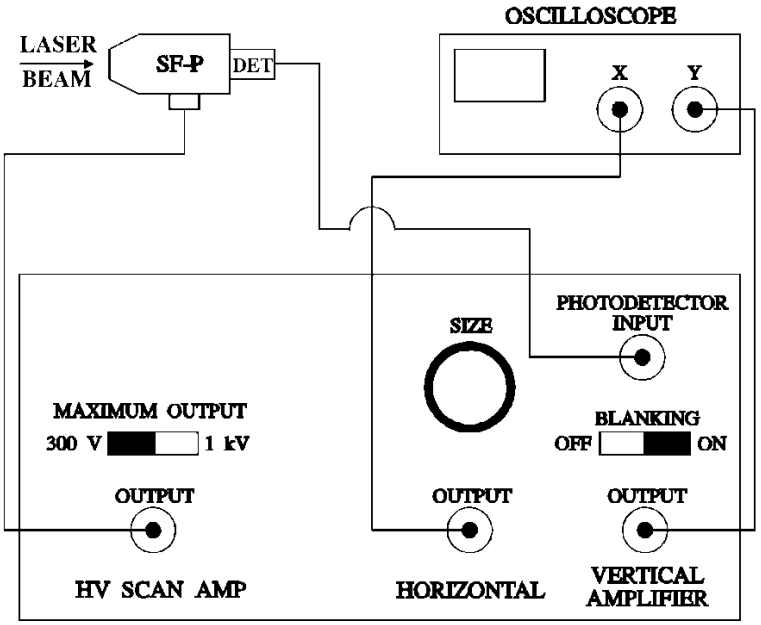

Figure 3.2: Electrical connections between the Spectra-Physics Model 470 Scanning Fabry-Perot Interferometer, the Hewlett-Packard Digital Oscilloscope, and the rear panel of the Spectra-Physics Model 476 Interferometer Driver.

the Driver high voltage output to the SF-P crystal input as indicated in Fig. 3.2, and reset the oscilloscope sweep to XY. (Press "Main/Delayed" and select "XY" in the screen menu.) Power **On** the Driver.

2. Set the Driver controls on the front panel:

   VERTICAL GAIN 100 with VARIABLE knob at mid-range
   SWEEP FREE RUN with TIME knob fully clockwise
   DISPERSION X2 with VARIABLE knob at mid-range
   CENTERING mid-range

3. Set the oscilloscope controls to:

   HORIZONTAL SWEEP XY
   X Gain 1 volt/div
   Y Gain 1 volt/div

4. Check again to see that the cable connections are as sketched in Fig. 3.2. Adjust the SIZE knob on the Driver rear panel so that the "non-blanked" portion of the oscilloscope sweep covers 10 divisions in the horizontal direction. The "non-blanked" portion is simply the raised portion of the displayed signal. The HORIZONTAL OUTPUT on the rear panel of the Driver is just an attenuated version of the high voltage ramp; the SIZE knob is a fine control on the attenuation factor. Be sure to understand what you're doing!

While you may already see a spectrum of the laser output displayed on the screen (see Fig. 3.3), you should now carefully center the laser beam on the SF-P aperture and align the beam with the optical axis of the SF-P. To do so, perform the following exercise.

5. Translate the SF-P horizontally and vertically using the translators on the optical rail rider. Make sure the laser beam enters cleanly the SF-P aperture. Now rotate the SF-P using the micrometer adjustments on the SF-P mount. Direct the beam reflected from the SF-P mirrors back toward the laser output. When the reflected beam hits the laser output mirror, the subsequent reflection from the laser mirror can be seen on the SF-P aperture. This "reflection of a reflection" indicates that the alignment is close enough. In fact, you may be too close, because light reflected from the SF-P back into the laser resonant cavity can interfere with and destabilize the radiation in the cavity.

By now you should see the spectrum of the laser output displayed on the oscilloscope. Two or three modes should be lasing under the Doppler-broadened profile of the neon transition, and this spectrum should appear twice because the scan includes more than one free spectral range of the SF-P. Fine-tuning the micrometer rotation adjustments should narrow the laser modes to essentially vertical lines.

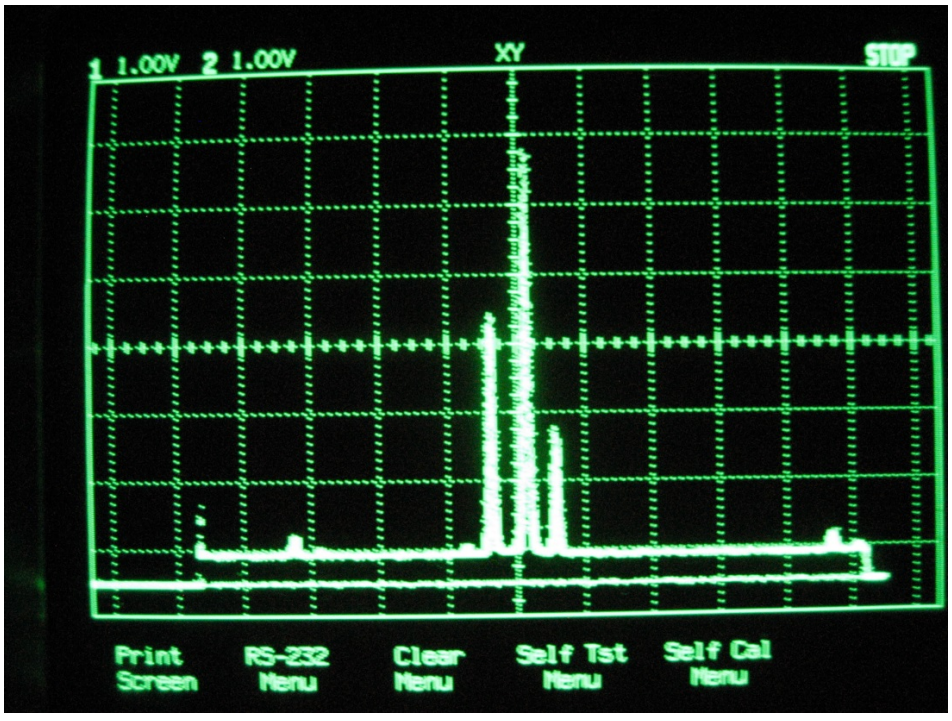

Figure 3.3: Photograph of the oscilloscope screen displaying three laser modes with a Doppler-broadened envelope. Just one free spectral range is shown.

We must discuss in more detail what is really meant by a "**free spectral range**" (FSR) in the context of a scanning interferometer. The multiple copies of the laser spectrum displayed on the oscilloscope screen are present because of the scanning feature of the SF-P. For a given wavelength λ, the condition for resonant transmission of a *confocal* SF-P is given by

$$d_{\mathrm{SF-P}} = d_0 = m\lambda/4 \tag{3.1}$$

where $d_{\mathrm{SF-P}}$ is the instantaneous mirror separation, m is an integer (e.g., 10^6), and d_0 is the mirror separation, let's say, at the beginning of a piezoelectric scan. As the piezoelectric drive increases the mirror separation, a resonant transmission occurs again at

$$d_{\mathrm{SF-P}} = d_0 + \Delta d^{(\mathrm{FSR})} = (m+1)\lambda/4 \qquad \Longrightarrow \qquad \Delta d^{(\mathrm{FSR})} = \lambda/4 \tag{3.2}$$

In other words, for a wavelength of 632.8 nm, transmission occurs each time the piezoelectric drive increases the mirror separation by 158.2 nm, a mighty small displacement. (Note that the factor of 4 in the denominators of Eq. (3.1) and Eq. (3.2) is replaced by a 2 for non-confocal interferometers, like a laser resonant cavity. While you should be able to justify the 2 by very simple physical arguments, the correction to 4 for a confocal cavity is a subtle point which you can use without deriving for now.)

The distance between copies of the laser spectrum provides a convenient calibration of the SF-P. We have just seen that the wavelength λ is transmitted when $d_{\mathrm{SF-P}} = d_0 = m\lambda/4$ and when $d_{\mathrm{SF-P}} = d_0 + \Delta d^{(\mathrm{FSR})} = (m+1)\lambda/4$, but it is also true that a longer wavelength $\lambda' \equiv \lambda + \Delta\lambda^{(\mathrm{FSR})}$ is transmitted when $d_{\mathrm{SF-P}} = d_0 + \Delta d^{(\mathrm{FSR})} = m\lambda'/4$. Combining the conditions

$$d_{\mathrm{SF-P}} = d_0 + \Delta d^{(\mathrm{FSR})} = (m+1)\lambda/4 = m\lambda'/4$$

with the definition $\lambda' \equiv \lambda + \Delta\lambda^{(\mathrm{FSR})}$ yields

$$\lambda = m\Delta\lambda^{(\mathrm{FSR})}$$

Substituting $m = 4d_0/\lambda$ from Eq. (3.1), we get

$$\Delta\lambda^{(\mathrm{FSR})} = \frac{\lambda^2}{4d_0}$$

It is convenient to express this result in terms of frequency:

$$\Delta\nu \approx \left|\frac{\mathrm{d}\nu}{\mathrm{d}\lambda}\right| \Delta\lambda \qquad \Longrightarrow \qquad \Delta\nu^{(\mathrm{FSR})} = (c/\lambda^2)\Delta\lambda^{(\mathrm{FSR})} = \frac{c}{4d_0}$$

The nominal mirror separation of our SF-P is $d_0 = 9.375\,\mathrm{mm}$, so that $\Delta\nu^{(\mathrm{FSR})} = 8.0\,\mathrm{GHz}$. We conclude that the distance between copies of the laser spectrum also corresponds to a frequency difference of 8.0 GHz which is called the "free spectral range" (FSR) of the SF-P. We shall make use of this number in our measurements with the SF-P.

The two or three active laser modes appearing on the oscilloscope screen usually drift back and forth under the Doppler profile of the neon transition, because the length of the laser cavity is thermally expanding and contracting. Recall from your reading in the references that the resonant wavelengths of the laser cavity (*not* a confocal arrangement) satisfy the relation $d_{\text{laser}} = m\lambda/2$ where d_{laser} is the mirror separation and m is an integer. The resonant frequencies are therefore $mc/2d_{\text{laser}}$, and hence the frequency separation of adjacent modes is $c/2d_{\text{laser}}$. The frequency separation $c/2d_{\text{laser}}$ is usually called the **mode spacing** or the **mode separation**, but can also be referred to as the free spectral range of the laser cavity. When the laser is first powered **On**, the plasma tube warms up, d_{laser} increases, and the allowed frequencies decrease in time. The result is a rather rapid movement of lasing modes under the Doppler profile whose center frequency is, of course, dependent only on atomic structure. When the laser reaches thermal equilibrium, the motion of the laser modes slows considerably. You may want to power the laser **Off** for a few minutes so that you can observe the warming effect when you power it back **On**.

If the Fabry-Perot is too well aligned, as mentioned above, you may see instability in the modes far beyond the smooth thermal effect described above. Deliberately misalign the interferometer slightly, if necessary, to keep light from reflecting back into the laser cavity and destabilizing the lasing action in this way.

3.2.1 Measuring the Mode Separation

Using the fact that the free spectral range (FSR) of the SF-P is 8 GHz, adjust the DISPERSION VARIABLE knob so that the laser spectrum repeats after 8 divisions on the oscilloscope horizontal scale; 1 division now equals 1 GHz. Measure the frequency separation of adjacent modes of the Model 1125P laser. The storage feature of the H-P 54603B oscilloscope provides a convenient method for measuring the frequency separation and obtaining a hard copy of the laser spectrum. Press **Stop** on the H-P oscilloscope, followed by **Erase**. The oscilloscope screen should now be clear. Press **Auto-store** on the oscilloscope and then quickly press **Stop**. A few traces of the laser spectrum should be superposed on the screen. A hard copy of this spectrum can be obtained on the Epson printer that is connected by serial port to the HP oscilloscope. The most efficient way to measure the mode separation is to employ the cursor features of the H-P oscilloscope. Use a sample variance technique to obtain an uncertainty for your measured value of the frequency separation. It may be useful to switch the Driver DISPERSION setting to $\times 5$ and $\times 10$, and use different portions of the piezoelectric length-versus-voltage curve. You will probably notice that the piezoelectric crystal has small nonlinearities in its length/voltage response. Do the best you can; all the random errors will be included in your sample uncertainty. *After* you have finished, compare your measured value with the nominal frequency separation quoted in the Uniphase Model 1125P Manual.

3.2.2 Measuring the Width of the Doppler Envelope

Also measure the apparent full-width-at-half-maximum (FWHM) of the Doppler envelope. Again use the storage feature of the H-P oscilloscope, but (Store) long enough to allow the thermal drift of the modes to trace out the Doppler envelope. Do not (Store) longer than necessary, however, as the slower thermal drift of the Fabry-Perot interferometer may complicate your measurements in that case. Again a sample variance technique will give you a good sense of your uncertainty. Interpret your measured FWHM in terms of a temperature for the helium-neon plasma. As we will derive (or have derived) in lecture,

$$\text{FWHM (in Hz)} = 2\sqrt{2\ln 2}\sqrt{\frac{kT}{m}}\frac{1}{\lambda}$$

Your deduced temperature will probably be below room temperature, indicating something is fishy. The resolution of this puzzle lies in the low level of pumping provided by the discharge through the plasma tube. The resonant modes of the laser cavity which lie in the wings of the Doppler profile don't have enough gain to actively lase. To put it another way, there aren't enough excited neon atoms with large velocities to enable the modes in the wings of the Doppler profile to provide enough gain to overcome the cavity round-trip loss. You are observing just the tip of the Doppler profile, and your measured FWHM is probably just the full width at 3/4 or 7/8 maximum. Examination of the Doppler profile near its base will reveal that, indeed, it is shaped like the cut-off top of a Gaussian rather than a full Gaussian. Unfortunately, we can't increase the plasma tube voltage (and hence current) to increase the number of excited neon atoms without damaging the power supply.

3.2.3 Measuring the Width of the Lamb Dip

As the active modes of the laser drift through the Doppler profile, you will notice that the amplitude of a mode dips slightly as it passes through the center frequency of the Doppler profile. The dip is called the Lamb dip, and is best observed by sweeping just one active mode through the Doppler profile by translating (usually piezoelectrically) one mirror. While there are two or three active modes in the Model 1125P laser, the effect is still rather obvious. When an active mode lies above the center frequency of the Doppler profile, the mode radiation field recruits photons from excited neon atoms by stimulating them to emit in the direction of their motion along the laser cavity axis (e.g., the z axis). Neon atoms with a range of velocities, $+v_z$ to $+v_z + \Delta v_z$, can contribute to the active mode, where Δv_z is determined by the contribution of collision and lifetime broadening to the total width of the neon transition. Collision and lifetime broadening are called *homogeneous* broadening mechanisms (which affect all atoms) and contribute much less to the total width of the neon transition than does the *inhomogeneous* mechanism of Doppler broadening (in which subpopulations of atoms participate). Moreover, neon atoms with velocities $-v_z$ to $-v_z - \Delta v_z$ can also contribute to the active mode, because the mode field can stimulate these atoms to emit photons along the negative z axis. Hence, two slices of the atomic velocity

distribution with total width $2\Delta\nu_z$ can contribute to the active mode when it lies above (or, by similar argument, below) the center frequency of the Doppler profile. However, as the mode approaches the center frequency, only atoms with velocities $-\Delta\nu_z/2$ to $+\Delta\nu_z/2$ can be stimulated to emit photons (in either direction). Hence the amplitude of the mode dips when it reaches the center frequency. See the references for more thorough discussions of the Lamb dip.

Measure the width of the Lamb dip. Again use the storage feature of the oscilloscope. The thermal drift of the laser modes should trace out the Doppler envelope complete with Lamb dip. You may have to turn the laser off for a few minutes and then turn it back on to increase the rate of thermal drift. As in the Doppler width measurement, remember that your goal is to observe the drift of the laser modes without letting the slower thermal drift of the SF-P complicate or wash out your measurements! As usual, use a sample variance approach. (This is not an easy measurement; expect 10% to 20% precision.) The mean lifetimes of the initial and final states of the 632.8 nm neon transition are approximately 100 ns and 10 ns, respectively. The corresponding contribution of lifetime broadening to the width of the transition profile is

$$\text{FWHM (in Hz)} = \frac{1}{2\pi}\frac{1}{10^{-8}\text{ s}} = 16\,\text{MHz}$$

From your measured width of the Lamb dip, does collision broadening contribute significantly to the homogeneous broadening of the neon transition?

Finally, place the polarizing prism between the laser and the SF-P and rotate it while you observe the amplitudes of the two or three active modes. You should see all of the active modes vary in amplitude together, because they are all polarized in the same plane. The Model 1125P probably uses a Brewster window on one end of the plasma tube to introduce losses for the unwanted polarization state. You will want to contrast this behavior with that of the modes of the "randomly" polarized Model 1125 laser.

3.2.4 Measuring the Polarization of the Uniphase Model 1125 Helium-Neon Laser

Carefully move the SF-P to the optical rail which supports the Model 1125 laser housed in the solenoid. See Fig. 3.4. The output beam of the Model 1125 is 5 mW and is "unpolarized". Repeat the alignment procedure and display the spectrum of the Model 1125 on the oscilloscope. Using the polarizing prism, examine the polarization of the active modes. (A quarter-wave plate for 633 nm is also available with the optical setup.) What do you see? Do you think that the output polarization of this laser should be described as "random"?

3.3 Measuring the Zeeman Splitting of Neon

In 1896 Zeeman observed that an atomic spectral line splits into several lines when the atom is placed in a magnetic field. We now know that the effect is due to the alignment of the atomic

magnetic dipole moment in the applied magnetic field. Initially the magnetic sublevels of the atomic states involved in the transition have the same energy (are degenerate), but when the field is applied the degeneracy is removed according to the Hamiltonian

$$\hat{H}_{\text{Zeeman}} = -\hat{\boldsymbol{\mu}}_{\text{atom}} \cdot \mathbf{B}_{\text{external}} \tag{3.3}$$

The atomic magnetic dipole moment is determined by the orbital and spin angular momenta of the electrons:

$$\hat{\boldsymbol{\mu}}_{\text{atom}} = -\sum_i \frac{g_l \mu_{\text{B}}}{\hbar} \hat{\mathbf{L}}_i - \sum_i \frac{g_s \mu_{\text{B}}}{\hbar} \hat{\mathbf{S}}_i \tag{3.4}$$

where the sum is over the electrons. Because the angular momenta are quantized, the dipole moment is quantized, and the magnetic sublevels separate into discrete energy levels. If we take the z axis to be along the magnetic field, the Zeeman shift of each magnetic sublevel can be written

$$\Delta E_{\text{shift}} = \langle n l j m_j | -\hat{\mu}_z B | n l j m_j \rangle = g m_j \mu_{\text{B}} B \tag{3.5}$$

(The result in Eq. (3.5) is *not* obvious; but a little group theory and quantum mechanics can be used to derive it.) In Eq. (3.5), g is called the "g-factor" (which is the same for all magnetic sublevels but may be different for different atomic states), m_j is the quantum number for the z component of the total angular momentum, and μ_{B} is the Bohr magneton. Transitions between

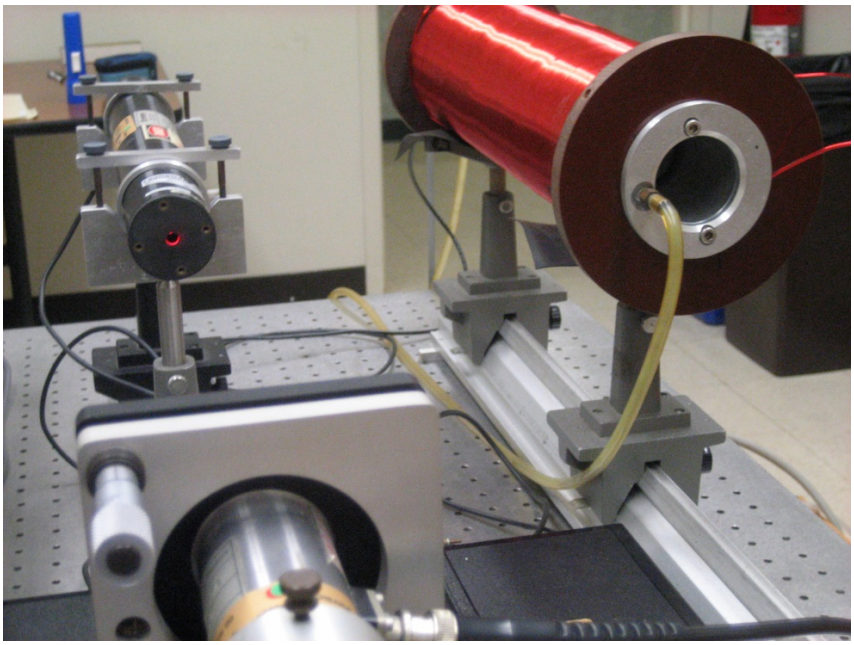

Figure 3.4: Photograph taken from the perspective of the Fabry-Perot interferometer (bottom-center-left). The Uniphase 1125P HeNe laser (top-left) illuminates the Fabry-Perot, and the solenoid (upper right) houses the Uniphase 1125 (unpolarized) HeNe laser.

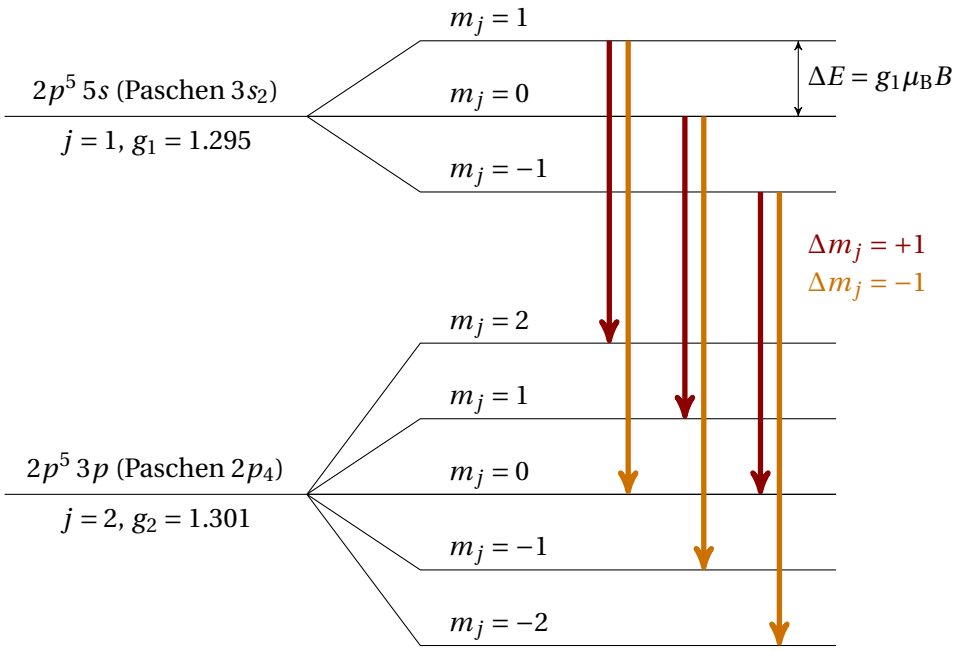

Figure 3.5: Zeeman splittings of the upper and lower Ne states involved in the 633 nm transition. The allowed transitions have $\Delta m_j = \pm 1$. Although the transitions with $\Delta m_j = 1$ have slightly different energy shifts from the energy in the absence of a magnetic field ($\Delta E/\mu_B B = \{g_1 - 2g_2, -g_2, -g_1\}$), our instrument cannot resolve these tiny differences. Curiously, if we average over the three transitions with $\Delta m_j = 1$ and compare to the average of the three transitions with $\Delta m_j = -1$, the splitting we observe depends only on g_2 of the lower lasing level.

different magnetic sublevels of the initial and final states result in the splitting of a spectral line into several lines, the number of lines depending upon the angular momenta of the initial and final states. See the reference by Eisberg and Resnick for an instructive treatment of the Zeeman effect in Na.

Ordinarily the observation of the Zeeman effect is an experimental *tour de force*. However, our scanning spherical-mirror Fabry-Perot interferometer has a resolving power of about 10^7 and allows us to observe the Zeeman splitting in neon with an applied magnetic field of just 500 gauss. For example, the Zeeman splitting between adjacent magnetic sublevels ($g\mu_B B$ in Fig. 3.5) corresponds to a frequency of 0.91 GHz with a magnetic field of 500 gauss. Futhermore, because we will be observing the laser beam traveling along the direction of the magnetic field, and because the selection rule $\Delta m_j = \pm 1$ applies, we will see the Doppler envelope split into two envelopes separated by twice the Zeeman splitting, or about 1.8 GHz at 500 gauss. See Fig. 3.5 for an example of the resulting transitions with an applied magnetic field.

The goal of this section of the experiment is to measure the Zeeman separation of the Doppler envelopes as a function of magnetic field. From this data, a value for g of the final state in the

633-nm transition can be deduced and compared with the literature value (1.301).

As a starting point, apply a magnetic field of about 500 gauss. The rear end of the laser head should be protruding about 3/4" from the rear end of the solenoid. This centers the lasing plasma in the solenoid and maximizes the spatial uniformity of the field. Use the HP 6574A Power Supply to generate a solenoid current of 10 A (the conversion factor is 49.9 gauss/A). Be sure to use the cooling water for the solenoid.

Caution

When using currents of 10 A or more, be sure to return the current to zero within one minute. Check the solenoid windings to make sure they are not hot. We don't want a melt-down! The power dissipated at 60 V and 20 A is 1.2 kW! Use the cooling water for the solenoid.

The instructions for using the HP 6574A are placed with the instrument.

At 10 A (499 gauss) you should see two Doppler envelopes that are fairly well separated, but the envelopes may not be perfectly symmetric. Any asymmetry in the Doppler profiles can easily lead to systematic errors in measuring the separation of the centers of the two envelopes. Previous students have found that symmetry is maximized when the separation of the envelopes is equal to an integer number of laser mode separations ($c/2d_{\text{laser}}$). This condition means that a Lamb dip occurs simultaneously in the two envelopes. It is suggested that you measure the Zeeman separation of envelopes at strengths of the magnetic field that yield symmetric envelopes.

You will probably find it convenient to normalize your measured Zeeman separation of envelopes by the laser mode separation. You can store a snapshot of the laser modes in one half of the H-P 54603B Digital Oscilloscope memory, and store a longer smear of the Doppler envelopes in the second half. Then you can use the oscilloscope cursors to measure both spacing and separation directly on the oscilloscope screen rather than dumping the screen to the Epson printer and analyzing the hard copy later. Of course you will probably want an occasional hard copy for your own records, but the transfer of the oscilloscope screen to the Epson printer is painfully slow (about 40 seconds). Use your time wisely.

Plot the Zeeman separation (expressed in mode spacings) versus solenoid current (or magnetic field). The slope of a linear fit of this plot can yield the g value for the final state of the 633-nm transition. Be sure to use a sample variance technique to determine uncertainties in the data, and propagate these uncertainties through to the value for g using a least-squares fitting procedure with a χ^2 criterion for goodness of fit.

3.3.1 More Advanced Measurements Using the Scanning Fabry-Perot Interferometer

The measurements described above serve as a great introduction to the use of our optical spectrum analyzer. However, there are many additional topics that can be explored with the same

basic experimental setup, and some may appeal to you as potential directions for a technical report. Here are some examples that you may wish to discuss with your instructor.

Polarization state of photons in the presence of a magnetic field When a magnetic field is applied along the axis of the "unpolarized" Uniphase 1125 HeNe laser, the output spectrum is split into two "Doppler envelopes", one of which is expected to be right-circularly polarized and the other left-circularly polarized. Measurements performed by Optics Lab students have revealed that the polarization state of one of the Doppler envelopes is well-described by mostly right-circular polarization with a little bit of left-circular polarization, and the other Dopper envelope is mostly left-circular polarization with a little bit of right-circular polarization. In each case the electric field of the small unexpected polarization is accompanied by a phase shift, and this phase shift seems to be a function of the strength of the applied magnetic field. It would be *very interesting* to see if the dependence of the phase shift on field strength is linear, as might be expected from the Faraday effect, perhaps due to circular birefringence of the neon plasma in the laser. This is a very intriguing, ongoing research project!

Transverse spatial modes of a laser A demonstration laser is placed with the experimental setup and can be used to investigate the transverse modes (TEM_{00}, TEM_{01} or TEM_{10}, TEM_{11}, etc.) of the laser beam. An intra-cavity iris diaphragm is an integral part of the laser resonant cavity, and when the iris is expanded, higher order spatial modes are allowed to lase, with energy distributed at greater radii from the optical axis. A fast silicon photodiode and an electrical spectrum analyzer are also available and can be used to measure the beat frequencies between the various transverse modes. This is a great visual *and* quantitative way to learn more about laser resonant cavities and their operation!

Nonlinear mode frequency pulling The HP electrical spectrum analyzer provides high precision measurements of the beat frequency between adjacent laser modes. It is possible to see that as a mode drifts toward the center of the Doppler envelope (toward the resonance frequency of the atomic transition), the frequency of the mode is pulled toward the resonance frequency. Physically, mode frequency pulling is due to the nonlinear change in the refractive index as the mode frequency approaches the resonance frequency of the atomic transition, and the change in refractive index causes a change in the wavelength associated with a particular frequency. Because a mode is defined by its wavelength (its wavelength must fit into twice the mirror separation an integer number of times), the frequency of a mode is seen to deviate in a nonlinear way from the frequency expected under the assumption of a constant index of refraction for the plasma filling the laser resonant cavity.

The effect leads to a dramatic shift in beat frequency depending on whether a mode lies exactly at the resonance frequency, with modes symmetrically situated on either side of it, or whether the resonance frequency lies midway between two adjacent modes. Using a beam splitter to send some laser light to the Fabry-Perot and the rest to the fast silicon detector and the HP spectrum analyzer, one can watch a fascinating transition from one

beat frequency when a mode lies at the center of the Doppler envelope, to another beat frequency when two adjacent modes lie symmetrically on either side of the center frequency. The difference in beat frequency is small — just 100 kHz out of 435 MHz, but the precision of the HP spectrum analyzer makes the shift in frequency easy to detect and display on the screen of the spectrum analyzer. It is truly mesmerizing! And a great study of resonance behavior at the atomic level!